The Fulnau landslide and former Lake Seewen in the northern Swiss Jura Mountains

Autor(en): **Becker, Arnfried / Davenport, Colin A. / Haeberli, Wilfried**

Objekttyp: **Article**

Zeitschrift: **Eclogae Geologicae Helvetiae**

Band (Jahr): **93 (2000)**

Heft 3

PDF erstellt am: **17.09.2024**

Persistenter Link: https://doi.org/10.5169/seals-168823

0012-9402/00/030291-15 $1.50 + 0.20/0
Birkhäuser Verlag, Basel, 2000

Eclogae geol. Helv. 93 (2000) 291–305

The Fulnau landslide and former Lake Seewen in the northern Swiss Jura Mountains

ARNFRIED BECKER[1], COLIN A. DAVENPORT[2], WILFRIED HAEBERLI[3], CONRADIN BURGA[3], ROGER PERRET[3], ALEXANDER FLISCH[4] & WALDEMAR A. KELLER[3]

Key words: Swiss Jura Mountain, stream gradient, landslide, rock fall, landslide-dammed lake, radiocarbon ages, palynostratigraphy, sedimentation rates

ABSTRACT

Investigations of the former lake at Seewen in the Canton of Solothurn, Switzerland, over the past 30 years have revealed a landslide history and a lake evolution during late Pleistocene and Holocene times. As the only Late Glacial lake known in the northern Jura Mountains, its existence has been documented by historical chronicles up to its final drainage in the late 16th century. Geological mapping indicates that former Lake Seewen originated when rocks from the *Homberg* Mountain slid into a river gorge near Fulnau and blocked the flow of the river Seebach. Age dating of the older lake sediments using radiocarbon and pollen indicates that this landslide happened around 13,000 to 13,500 BP. The lake extended upstream in an easterly direction reaching its maximum extension in the late sixth or early seventh century AD. Although the lake sediments reach a thickness of more than 23 m above debris deposits, the water depth appears to have been limited to not more than 10 m. These lake sediments are highly cohesive, rich in clay and organic matter with silty layers. X-ray investigations revealed the existence of numerous "dropstones" in Late Glacial deposits. Holocene sedimentation took place at rates averaging 1.5 mm/a back to 7,000 BP and 2.6 mm/a between 7,000 and 9,000 BP, whereas the Late Glacial sedimentation rates are somewhat lower at 2.1 mm/a. Thin silty-sandy layers allow a correlation of different drill cores and indicate short-term changes in the sedimentation conditions which might be triggered by exceptional flood-events, storms, subaquatic slumping or earthquakes.

ZUSAMMENFASSUNG

Untersuchungen am ehemaligen Seewener See im Kanton Solothurn, Schweiz, über einen Zeitraum von 30 Jahren konnten die Geschichte dieses Bergsturz-Stausees und seine Entwicklung während des späten Pleistozäns und im Holozän aufklären. Als einziger bekannter spätglazialer See im nördlichen Jura ist seine Existenz durch schriftliche Dokumente bis zu seiner endgültigen Trockenlegung im späten 16. Jahrhundert belegt. Geologische Kartierungen belegen, dass der ehemalige Seewener See durch Felsmassen aufgestaut wurde, die vom Homberg in die Schlucht nahe Fulnau glitten und dort den Seebach blockierten. Datierungen der ältesten lakustrinen Sedimente mit Hilfe der Radiokarbonmethode und der Palynostratigraphie weisen auf ein Alter für den Bergsturz von ungefähr 13,000 bis 13,500 BP hin. Der See erstreckte sich in östlicher Richtung und erreichte im späten 6. oder frühen 7. Jahrhundert n. Chr. seine maximale Ausdehnung. Obgleich die Seesedimente eine Mächtigkeit von mehr als 23 m über basalem Schutt erreichen, scheint die Wassertiefe 10 m nicht überschritten zu haben. Die Seeablagerungen sind stark kohäsiv, reich an Ton und organischem Material und enthalten siltige Lagen. Röntgenuntersuchungen belegen zahlreiche «Dropstones» in spätglazialen Ablagerungen. Die Sediemntationsraten im Holozän lagen im Mittel bei 1.5 mm/a bis ca. 7,000 BP und 2.6 mm/a zwichen 7,000 und 9,000 BP, im Spätglazial bei 2.1 mm/a. Dünne siltig-sandige Lagen ermöglichen eine Korrelation der verschiedenen Bohrkerne und weisen auf eine kurzfristige Änderung in den Sedimentationsbedingungen hin, die durch aussergewöhnliche Flutereignisse, Stürme, subaquatische Rutschungen oder Erdbeben erklärt werden können.

Introduction

Former Lake Seewen in the Canton of Solothurn, some 15 km to the south of Basle in the Jura Mountains of northern Switzerland and close to the eastern margin of the Upper Rhine Graben, was formed by the Fulnau landslide (Haeberli et al. 1976), when masses of Jurassic limestone slid down the northern slope of the *Homberg-Wisig* anticline in prehistoric times (Fig. 1). The first historically verified attempts to drain the lake date back to the year 1488 AD (Annaheim & Barsch 1963). Towards the end of the 16th century the 260 m long *See-loch* gallery was built in limestones at *Welschhans* on the northern flank of the Seebach valley, which led to the complete drainage of the lake. Successful cultivation of the flat, roughly 2.5 km long, valley floor was only made possible in 1919 with the correction of the Seebach river and the artificial drainage of the water-saturated soils (Annaheim & Barsch 1963).

Detailed scientific research started in the 1970s with seismic refraction soundings, exploratory core drilling and pollen

[1] Institut für Geophysik, ETH-Hönggerberg, CH-8093 Zürich, Switzerland
[2] School of Environmental Sciences, University of East Anglia, Norwich NR4 7TJ, England
[3] Geographisches Institut, Universität Zürich, CH-8057 Zürich, Switzerland
[4] EMPA, CH-8600 Dübendorf, Switzerland

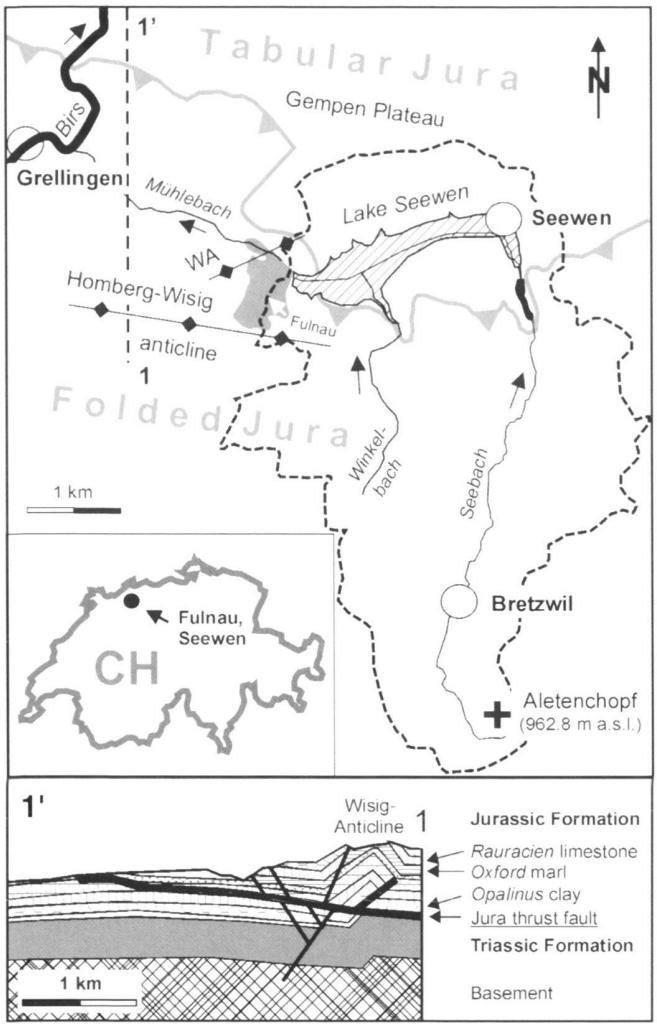

Fig. 1. Location map of geological and drainage features of the Lake Seewen catchment area (indicated by dashed line). WA = Welschhans anticline. Section line 1-1' is a N-S geological cross-section illustrating the regional structure (after Laubscher 1998).

analysis to determine the geometry, characteristics and approximate age of the sediment fill covering the limestone bedrock (Haeberli et al. 1976). The results of these studies suggested that sedimentation had started in late Pleistocene to early Holocene times in a landslide-dammed lake. River erosion, inherited tectonic structures and degradation of Pleistocene permafrost has been envisaged as possible trigger mechanisms for the landslide.

Pleistocene lakes and lake sediments are known from several places in the Jura Mountains where karst drainage was impeded by permafrost in an environment of harsh periglacial conditions (Barsch 1968; Frenzel et al. 1992). The general predominance of karst drainage under warm Interglacial or Holocene conditions, however, prevented such lakes from persisting and other lakes from being created. The sedimentary record of former Lake Seewen, therefore, provides a rare opportunity for reconstructing the regional vegetation history after the coldest periods of the last Ice Age and analysing Holocene landscape evolution as influenced by early man (Burga & Perret 1998). Additionally, the proximity of Lake Seewen to the tectonically active Upper Rhine Graben provides the opportunity for detecting sediment-preserved signals of strong earthquakes such as the one which destroyed the city of Basle in 1356 AD.

In September 1997, a new survey of systematic core drilling and sediment analyses commenced with a commercial ramcore borehole located at the presumed deepest point of the lake (SR1 in Fig. 2). This borehole and those drilled in February 1998 with a Livingstone probe from the University of Berne (SL2 to 4 in Fig. 2) provided information about basin geometry and lateral variations in sedimentation. This paper describes these investigations and the results of detailed sediment analyses and age dating of the lacustrine sediments of the former Lake Seewen, and the geological/geomorphological mapping of the Fulnau landslide.

Geological setting and drainage

The former Lake Seewen and the Fulnau landside are located along the border of the Folded Jura to the south, and the Tabular Jura in the north (Fig. 1 and 2). The transition from Folded to Tabular Jura and the main fold structure are shown in the cross-section (Fig. 1). The Gempen-Plateau of the Tabular Jura north of Lake Seewen is a limestone plateau, with a gentle dip of 1 to 2° to the south (Bitterli-Brunner & Fischer 1988). Only at the southern rim of the Plateau is there a general increase of the dip of the limestones, where dips of up to 25° can be seen. To the south and southeast of the former Lake Seewen, the Folded Jura is thrust onto the Tabular Jura, and to the southwest and west the Folded Jura is characterized by the two anticlines of *Homberg-Wisig* and *Welschhans* (Fig. 3). The *Homberg-Wisig* anticline is a major WNW-ESE trending structure of the northern Folded Jura, which is presumed to have been generated above a pre-existing flexural monocline (Fig. 1) in late Miocene times (Laubscher 1998). In contrast, the *Welschhans* anticline is a subordinate WSW-ENE striking structure with a total shortening of 50 m or even less (Laubscher 1998). Both these structures contribute important boundary conditions for the Fulnau landslide and are discussed in more detail later.

The Upper Jurassic limestones, which are the dominant lithology in the surroundings of former Lake Seewen, may be locally karstified. However, the limestones seen at the western end of the former lake do not contain large-scale karst features and the lake basin is generally free of karst phenomena with the exception of the small ponor of *Hägenloch* (Fig. 2). Therefore, whilst the possibility of direct loss of water from the former lake into karstified bedrock has to be taken into account during lake evolution, such losses are considered to be minor.

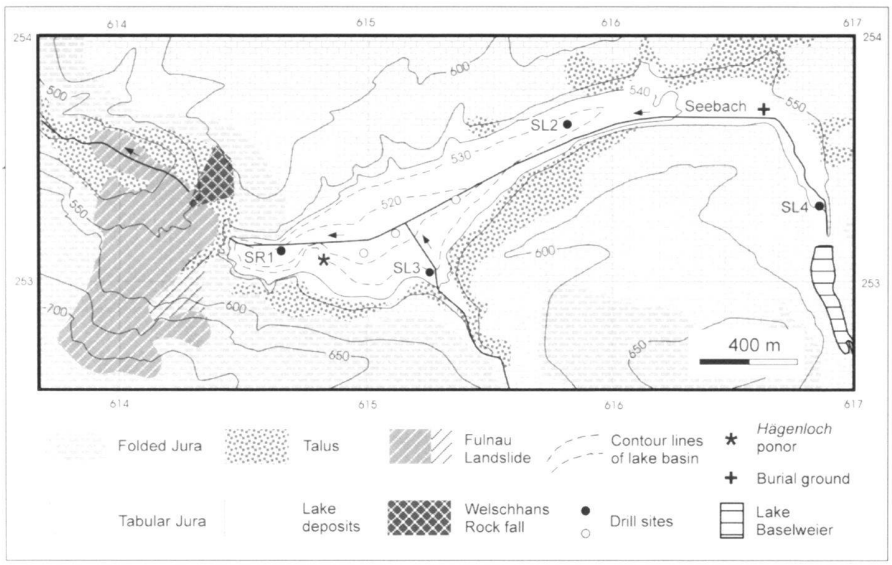

Fig. 2. Simplified geological map of the present-day Lake Seewen basin and Fulnau area.

Former Lake Seewen belongs to the Seebach drainage system. The most important tributaries of Lake Seewen are the Winkelbach (or Homberggraben, Hombergbächli) and the river Seebach itself, within a catchment area of 18 km^2 (Fig. 1). The headwaters of Seebach river are some 6 km to the south of Lake Seewen where they spring at an altitude of around 900 m a.s.l. close to the *Aletenchopf* mountain (Fig. 1). The river Seebach (or Mühlebach, which is synonymous for the lower course of the river Seebach) joins the river Birs near the village of Grellingen (Fig. 1) at an altitude of 310 m a.s.l. Thus, the river Seebach descends by approximately 600 m along its course of 12 km, equivalent to an average stream gradient of 50‰. A more detailed examination of the stream gradient, based on topographic maps at a scale of 1:25000, reveals a clear subdivision of the course into the upper reaches between the village of Bretzwil and the western end of former Lake Seewen (Fig. 1 and 4), and the lower reaches (the Mühlebach section) between the western termination of the former Lake Seewen and the river mouth near Grellingen (Fig. 1 and 4). The upper course stream gradients reach maximum values of 20 to 25‰ near Bretzwil, decreasing downstream towards Seewen at values of 15 to 20‰ . The natural course of the river Seebach is strongly disturbed due to the constructed dam and reservoir of the Baslerweier and a culvert in the village of Seewen. Moreover, in the area of former Lake Seewen, the channel of the river Seebach is completely artificial. An estimate for the natural gradient at the base of the sedimentary lake basin fill can be given with 13 or 14 ‰, which would lie within the trend of the stream gradient values of the upper course (Fig. 4). After passing through the *Seeloch* gallery at the western end of former Lake Seewen and the artificial channel, the natural lower course of the Mühlebach section begins. This section is characterized by much higher stream gradient values compared to the upper reaches, ranging from 35 to155‰. The western termination of former Lake Seewen and the Fulnau landslide lies close to the knickpoint of the stream gradient. Because former Lake Seewen is a landslide-dammed lake, it is reasonable to assume that backward erosion of the River Mühlebach created conditions for slope instabilities in the Fulnau area, leading to the landslide and the blockage of the Seebach drainage system. The knickpoint and the associated changes in the gradient on this scale are unlikely to have been caused by the landslide or to be post-landslide in age.

Fulnau landslide

Geology of the Fulnau area

The geology of the Fulnau landslide and the surrounding area is shown in Figs. 5 and 6. The dramatic widening of the Mühlebach valley occurs near to Fulnau where the river Seebach cuts through the small *Welschhans* anticline. The ENE-WSW trend of the axis of this anticline (Laubscher, pers. comm.) (Fig. 3) can be inferred by the strike and dip of layering along the northeastern and southwestern margin of the valley (Fig. 5). During backward erosion of the northwestern limb of the anticline by the Mühlebach river, oversteepened rock faces collapsed and successive erosion removed the core of the anticline. This limb of the anticline can be inferred from the topography, that is, the narrowing of the valley slopes, which are crowned by steep cliffs (Fig. 3), and also by the increasing stream gradient (104 and 113‰), as the river passes over the harder limestones (Fig. 4). In the core of the *Welschhans* anticline, softer *Oxford* marls are exposed (Laubscher, pers. comm.), frequently covered by debris and, thus, difficult to recognize in the field. The northern margin of the valley is well marked by the rock cliffs above the main Grellingen-Seewen road (Fig. 3, 5). North of that road, rock is exposed, at least as

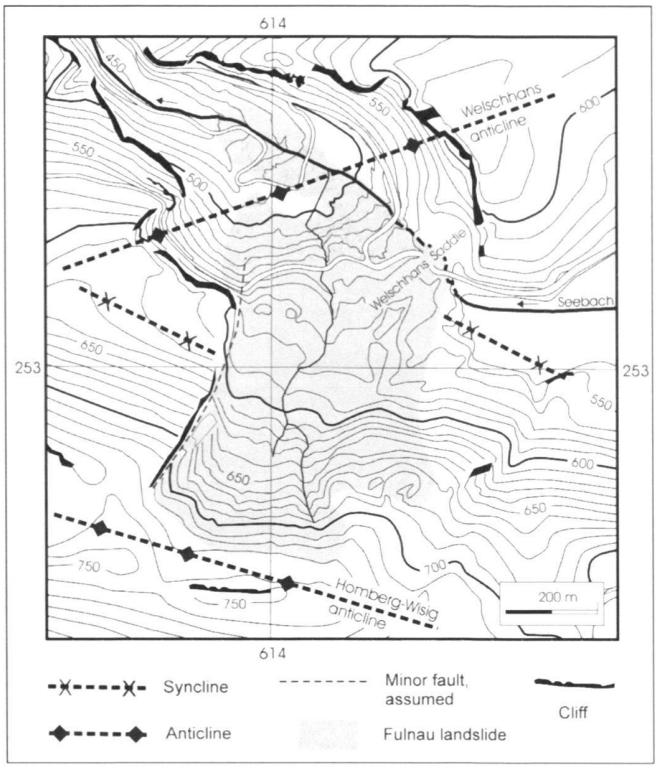

Fig. 3. Topographic map of the Fulnau area including major geological structures.

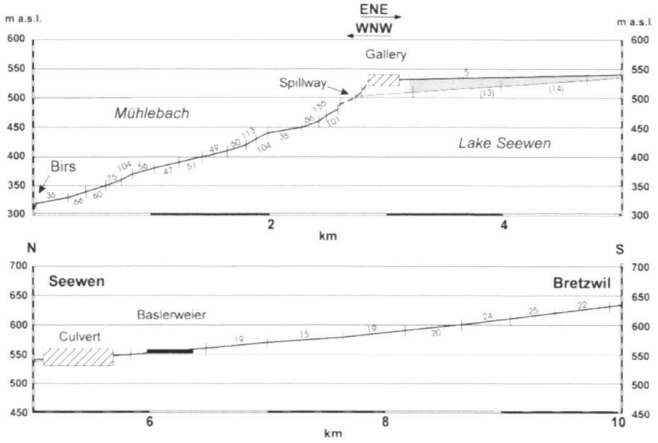

Fig. 4. Stream gradient profile (in two parts) of 10 km length along river Seebach between Bretzwil and the Birs junction. [Gradients are shown in parts per thousand = ‰]

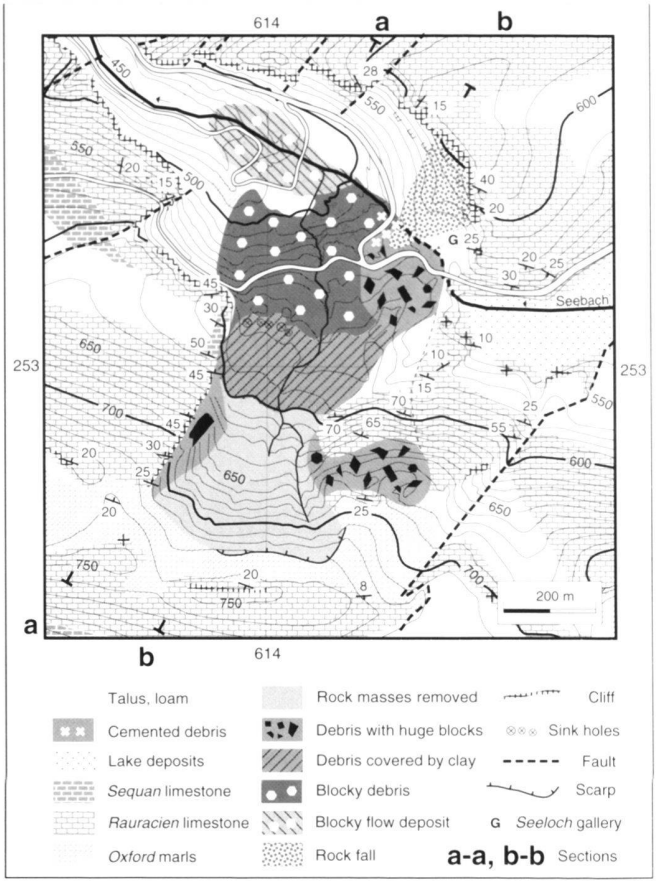

Fig. 5. Geological map of the Fulnau area. The stratigraphic sequence of the bedrock is from *Oxford* marls at the base to *Sequan* limestones at the top (Oxfordian, Upper Jurassic). Sections **a** and **b** are given in Fig. 6.

far to the south as the *Seeloch* gallery (G in Fig. 5), which has been built almost entirely in rock (Moser, pers. comm.). Here, the rock surface must be covered only by thin debris, because the two portals of the gallery have an elevation of 535 and 525 m a.s.l. and the crest of the *Welschhans* saddle between former Lake Seewen and the Mühlebach valley has an altitude of only 551 m a.s.l. The continuation of *in situ* rock can be seen along the western and southwestern end of the lake basin, largely as almost continuous exposures of flat-lying or gently dipping *Rauracien* limestones (Fig. 5). It seems there can be only a small notch very close to the portal of the *Seeloch* gallery, where the river originally flowed through the rock bar at the western end of the lake basin. This gorge-like feature is located close to the axis of a syncline, defined by south-dipping *Rauracien* limestones to the north, north-dipping limestones to the south and flat-lying limestones at the western extension of the lake basin (Fig. 5). These observations suggest that there was a largely intact rock bar at the western end of the lake basin through which the river Seebach must have discharged either through a gorge or a karst-enhanced pathway before the Fulnau landslide event. Overall, the upper Mühlebach valley can be described as a *'half-klus'*, where the *Welschhans* anticline has one broken limb (W), one largely intact limb (E) and an excavated core.

The structure of the *Homberg-Wisig* anticline can be best seen along a NNE-SSW profile west of the Fulnau landslide

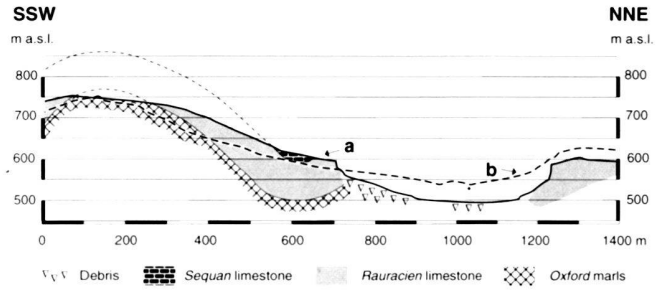

Fig. 6. Geological cross-section (a) W of the Fulnau landslide and topographic section (b) through the landslide. For the position of the section lines see Fig. 5.

(Fig. 3, 5, 6). Along the western scarp bounding the Fulnau landslide, the strike and dip of the *Rauracien* limestones can be easily measured. Additionally, at the crest of the anticline, *Oxford* marls are exposed, which permits the mapping of the contact with the overlying *Rauracien* limestones (Fig. 6). The thickness of the *Rauracien* limestones used for the construction of the cross-section is taken to be 90–100 m (Koch et al. 1936). The cross-section in Fig.6 shows simple folding, with the *Homberg-Wisig* anticline in the south complemented by a small syncline immediately to the north. Both structures have an axial trend of about 110°. The crest of the *Homberg-Wisig* anticline has been eroded, so that *Oxford* marls are exposed along the fold saddle: this is the same marl that is exposed in the Mühlebach valley. The core of the small complementary syncline contains *Sequan* limestone. The dip angle of the base of the *Rauracien* limestone is, with the exception of the hinge zones of the anticline, always larger than the natural slopes of the mountain flank. This relationship, together with the core of the small syncline acting as an abutment at the bottom of the slope, provides stable slope conditions. Therefore, in most parts of the anticline where these conditions are preserved, landsliding simply by bedding-plane parallel slip of the *Rauracien* limestones on the *Oxford* marls cannot take place.

Immediately east of the Fulnau landslide, the *Rauracien* limestones seem to be disturbed, as indicated by the extraordinary dip values of up to 70°, which are not normal for the *Homberg-Wisig* anticline (Laubscher, pers. comm.). This observation, together with a chaotic block field higher up the slope, suggests that this part of the *Homberg-Wisig* anticline has been affected by the slope movements, most likely as block rotations. Additionally, the small syncline at the foot of the *Homberg* mountain cannot be traced directly across the landslide area to the eastern flank. Although the strike of this syncline is approximately the same as that of the small syncline at the western end of the lake basin (Fig. 3), the position of the fold axis suggests a sinistral offset in the range of 250 to 300 m. In the absence of evidence for the existence of a 'fold bend', a 'fold jump' or a fault, their relationship remains problematic. However, NE-SW striking faults are common in the area and many are older than the Folded Jura. From regional mapping, most of them are Eocene to Oligocene in age, are normal faults with a throw of generally less than 100 m, and some of them can be traced into the Folded Jura (Buxtorf 1901; Laubscher 1998; Senn 1928). Two important normal faults can be seen east and west of the Fulnau landslide (Fig. 5), which can be followed from the Gempen Plateau of the Tabular Jura for some distance into the Folded Jura. A similar fault of more limited extent may be responsible for the scarp on the western edge of the landslide and could have facilitated a sinistral offset of the syncline.

Geology of the Fulnau landslide

The head of the Fulnau landslide is at an altitude of 730 m a.s.l., which is clearly marked by a small scarp in the *Oxford* marls (Fig. 5). The toe of the landslide in the Mühlebach valley lies at an altitude of about 460 m a.s.l. Thus, the maximum height is about 270 m and the maximum length is about 1150 m.

The landslide area can be subdivided into (1) scar areas where most of the unstable rock masses were removed, (2) disturbed areas with indications of limited block motions, and (3) main accumulation areas. Between an altitude of 730 and 600 m most of the limestone succession was removed (Fig. 5). Above 650 m, the *Oxford* marls outcrop and further down the slope the unmoved limestones are covered by a thin veneer of debris of mainly *Oxford* marls. An area with indications of limited motions is believed to be seen in the huge blocks (exceeding 15 m edge length) seen at the Grellingen-Seewen road bend (Fig. 5). Many blocks show intact bedding planes with dips of less than 20°, which is similar to the dips seen in the *in situ* limestones in the immediate vicinity. An area with indications of down-dip motions of large blocks over short distances can be seen at an altitude of between 640 and 680 m a.s.l. on the eastern side of the landslide (Fig. 5). Below this area the *Rauracien* limestones dip steeply (up to 70°) and are seen to be largely intact (Fig. 5). Moreover, above the area of debris with large blocks (chaotic block field) seen on the eastern side of the landslide and within not more than 100 m at the top of the slope there are *Oxford* marl outcrops (Fig. 5). This observation indicates that the chaotic blocks cannot have been transported for any significant distance. Adjacent to the western scarp of the Fulnau landslide is a similar area with huge blocks showing signs of limited motions (Fig. 5). Most obvious is a giant block (almost a 100 m in length), which exhibits bedding planes with an orientation of 130-135/35N, being very similar to the layering seen in the rocks of the cliff close to the block, i.e. 100-110/30-45N. Furthermore, a fissure up to 3 m wide splits the block in a N35E direction. Another fissure with a 140/60S orientation can be traced across the N35E striking fissure, showing only a minor sinistral offset of around 1 m. The location and the slight change in dip is consistent with small movements and only slight rotation during downslope sliding and tilting.

There are three main accumulation areas: a "toe" (shown as "blocky flow deposits" in Fig. 5), following more or less the

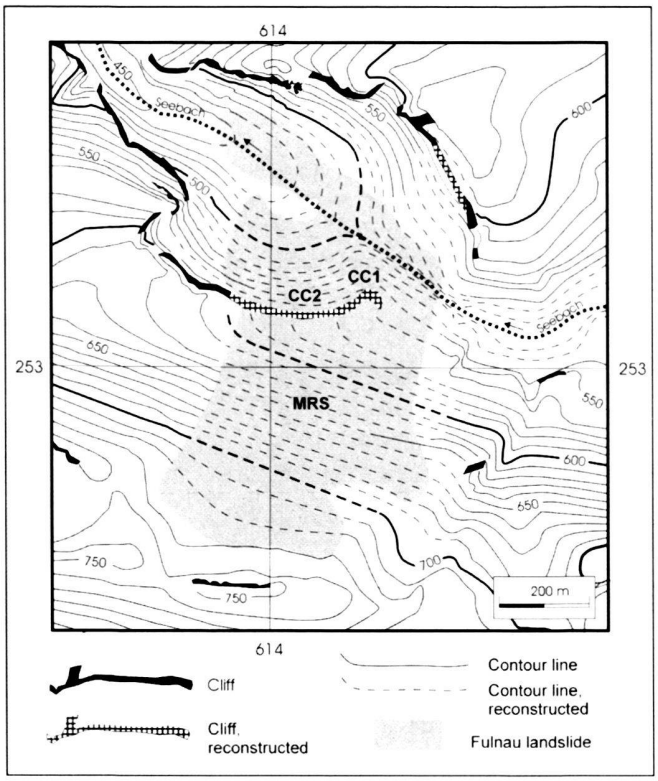

Fig. 7. Reconstructed pre-landslide topography of the Fulnau area. CC1 and CC2 show the conjectured position of the 'cliff-line collapses'. MRS = 'main rock slide' area.

deepest part of the Mühlebach valley; a "debris fan" (shown as "blocky debris" in Fig. 5) above the toe; and a "hummocky terrain" (shown as "debris covered by clay" in Fig. 5) between an altitude of 600 and 570 m a.s.l. The toe and the fan are characterized by debris containing big blocks, which show clear signs of tumbling, i.e. highly variable bedding dips. These blocks are concentrated especially in the toe region south of the river Seebach, in the fan region west of the road bend and along the border to the hummocky terrain to the south. Lithologically, there is no difference between the toe and the fan. It is possible that the toe followed the former thalweg of the river Seebach and so water may have had a stronger influence on toe formation compared with the fan. Certainly, the small exposures of debris seen in the river banks at the downstream limits of the toe reveal gravel size fragments in a loose matrix, similar to a saturated flow deposit. The hummocky area is a meadow divided by a small brook into two nearly equal-sized terrains with no indications of large blocks at the surface, which is in clear contrast to the rugged terrain of the fan and toe areas. West of the brook, along the northern rim of the hummocky area close to the first of the large blocks of the fan area, five depressions with a diameter of a few metres and a depth of 1-1.5 m can be seen (Fig. 5). Because of the general lack of large-scale karst features in the surrounding limestones, these depressions are considered to be sink holes created by subsurface erosion (piping). 'Sink hole' formation involves the washing out of fine-grained silty-sandy material in a blocky matrix resulting in cavities which eventually collapse and reach the surface. It is believed that these conditions are best fulfilled in the "hummocky terrain" close to the edge of the "debris fan" where a line of depressions can be seen in the meadow.

Palaeotopography and succession of sliding events

A reconstruction of the palaeotopography of the Fulnau area before the landslide is given in Fig. 7. It is assumed that the slope angle of the talus along the steep cliffs of the Mühlebach *half-klus* is not greater than 30°, consistent with the presence. Additionally, the depth of the former thalweg of the river Seebach in the western part of Lake Seewen is known from a seismic survey (Haeberli et al. 1976). Furthermore, the *Seeloch* gallery is sited in bedrock. Finally, the contour lines on either side of the landslide scar can be matched, interpolating the simple topography of the northern flank of the *Homberg* mountain. The cliff along the western edge of the landslide did not exist, because it is a scar caused by the landslide itself. A slight modification of the cliff along the northern margin of the *half-klus* is necessary because of a later rock fall. The most conservative location and trend of the cliff at the foot of the landslide is shown, but it is possible that this cliff lay further south and/or to the east. Two main former cliff areas are distinguished (CC1 and CC2 in Fig. 7) which are considered to be the locations of the initial slope collapses which facilitated the main rock slide (MRS in Fig. 7).

In this reconstruction of the palaeotopography, the eastern flank of the *half-klus* is at an early stage of dissection by the river Seebach, creating a gorge-like feature. Based on the geological arguments presented earlier, the northern flank of the gorge along the right side of the river must have been steep. The appearance of the southern flank of the gorge is not very well constrained, because it depends largely on the trend of the cliff. Certainly, it was also a steep flank, at least in part. Overall, the evidence suggest the presence of a narrow pre-landslide gorge, about 200 m long and 20-30 m deep, where the river Seebach descends into the *half-klus* (Fig. 7).

Somewhere along the gorge, in its central or western section, the river Seebach would have cut down to the base of the *Rauracien* limestones at about 510 m a.s.l., exposing the *Oxford* marls. These conditions would have been crucial for the initiation of the Fulnau landslide sequence, by providing the opportunity for the undercutting of the limestones by erosion and the weakening of the abutment of the northern slope of the *Homberg* mountain. The sequence of events required to explain these landslide features is given in Fig. 8. Event 1 probably started with the toppling and sliding of huge blocks from the edge of the gorge (CC1 in Fig.7) along the slightly N- dipping top of the *Oxford* marl, blocking the flow of the Seebach river. Below the gorge, the larger blocks tumbled to form a

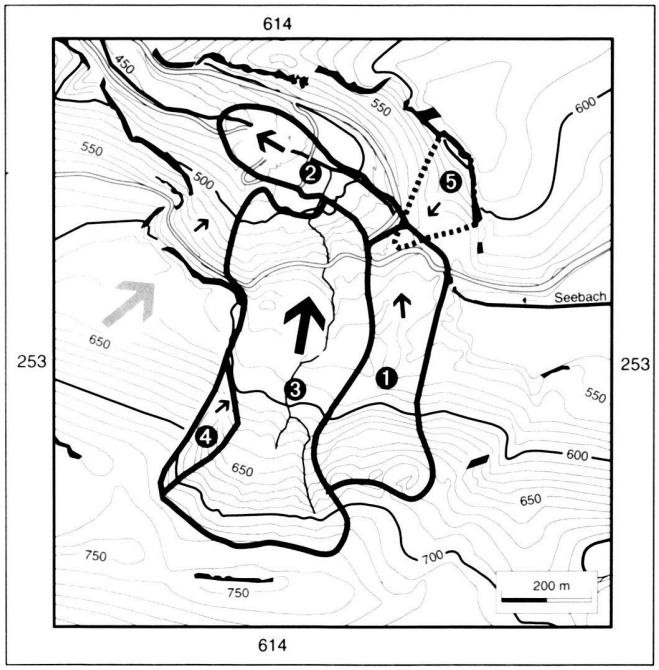

Fig. 8. Conjectured landslide and rock fall sequence (1 to 5) of the Fulnau area. Arrows indicate the direction (black) or possible direction (grey) and the size of the arrows indicates the relative distances of mass movements.

more chaotic deposit which rapidly separated into finer materials downslope, becoming a debris flow from the mixture of fine debris and water (shown as event 2 in Fig. 8). As a result of the cliff collapse, the whole uphill part of the limestone mass of the *Homberg-Wisig* anticline to the south started to slide northwards for a short distance, maybe 100 m, remaining more or less intact. Where the limestone unit thinned out and, thus, the basal frictional resistance increased, i.e. close to the top of the anticline, these motions created the chaotic block field. At this point, due to the failure of the remainder of the abutment (CC2 in Fig. 7) and the downslope mass movements of landslide event 1 (Fig. 8), the main part of the Fulnau landslide (MRS in Fig. 7) became mobilized (event 3 in Fig. 8), removing rocks from the flank of the *Homberg* mountain and depositing them in the Mühlebach valley. Sometime afterwards, huge blocks along the newly formed western cliff of the rockslide (MRS) separated with limited movement, so that they remained high on the slope (event 4 in Fig. 8). After the emplacement of the landslide debris, erosion of the newly exposed *Oxford* marl surface high up on the slope became possible and this eroded marl material, together with some remaining limestone debris, may have accumulated downslope partly covering earlier landslide debris to form the 'hummocky area'.

Based on the palaeotopographic reconstruction (Fig. 8) and on an assumption that most of the limestones and parts of the *Oxford* marls were mobilized during the Fulnau landslide, an upper limit of $14 \cdot 10^6$ m^3 can be estimated for the volume involved. A reasonable estimate of the lower limit can be based on the minimum height/length (H/L) ratio approach, the so-called fahrböschung (angle of reach) for unobstructed moderately large landslides using the approach of Corominas (1996) which is based on 204 landslides of all types. The H/L ratio for the Fulnau landslide is 270 m/1150 m = 0.23478 which gives a volume in the range of $7 \cdot 10^6$ m^3, similar to that given by Haeberli et al. (1976) using a simple geological block failure model. Because the main source of uncertainty of the volume estimates arise from geological assumptions, a realistic estimate would be not much higher than the lower limit, probably no more than 10^7 m^3.

It is believed that the Fulnau event was not very energetic, because there is no evidence of run-up in front of the main landslide area, there being only the small debris flow in the centre of the valley. The only debris seen on the northern slope of the *half-klus* has accumulated by rockfall from the cliffs north of *Welschhans* saddle (5 in Fig. 8) and, as it appears, is not part of the Fulnau landslide.

The age of the Fulnau event cannot be established directly. Datable organic material, such as palaeosols and plant remains, need to be found below the toe where the former valley floor has been covered by landslide debris. However, because the landslide dammed the gorge, the minimum age of the Fulnau event can be established indirectly by dating the oldest deposits in the former Lake Seewen.

Former Lake Seewen

Despite the fact that Lake Seewen no longer exists, the morphology of the valley with the flat ground west of the village of Seewen gives a clear impression of the existence of a lake in earlier times. The lake basin extends over a distance of about 2.5 km, starting at the northern termination of the constructed Baslerweier impounded reservoir, extending northwards beyond the village of Seewen, and turning westwards to end east of the *Welschhans* saddle, i.e. the rock bar at the western end of the former lake. The maximum width of the lake is approximately 500 m (Fig. 2). The lake basin has been the target for two research programmes: the first, initiated by the University of Basle in the 1970s, involving a refraction seismic survey, three ram boreholes and the first palynostratigraphic investigations; the second, a still ongoing research project of the ETH Zurich in cooperation with the Universities of Zurich, Berne and East Anglia. This later study includes ram and Livingstone drilling at a further 4 sites, sediment analyses, palynostratigraphy and extensive radiocarbon dating (Fig. 2).

Geophysical investigation and lake basin geometry

In February, 1974, a refraction seismic survey using explosives was carried out along several profiles, total length 3460 m, in the western lake basin by the University of Basle (Haeberli et

Table 1. Summary of drilling programme.

Drill Hole	Swiss geograph. Co-ordinates	Maximum Depth (m)	Core Diameter (mm)	Thickness of Lake Deposits (m)
SR1	614.653/253.103	26.77	100	23.63
SL2.1	615.812/253.634	6.83, 9.76	80, 50	9.45
SL2.2	615.812/253.634	7.52	80	?
SL2.3	615.812/253.634	7.47	80	?
SL3.1	615.244/253.038	3.58	80	3.50
SL3.2	615.244/253.038	4.21	80	3.70
SL3.3	615.244/253.038	3.54	80	?
SL4	616.840/253.305	1.48	80	0.98

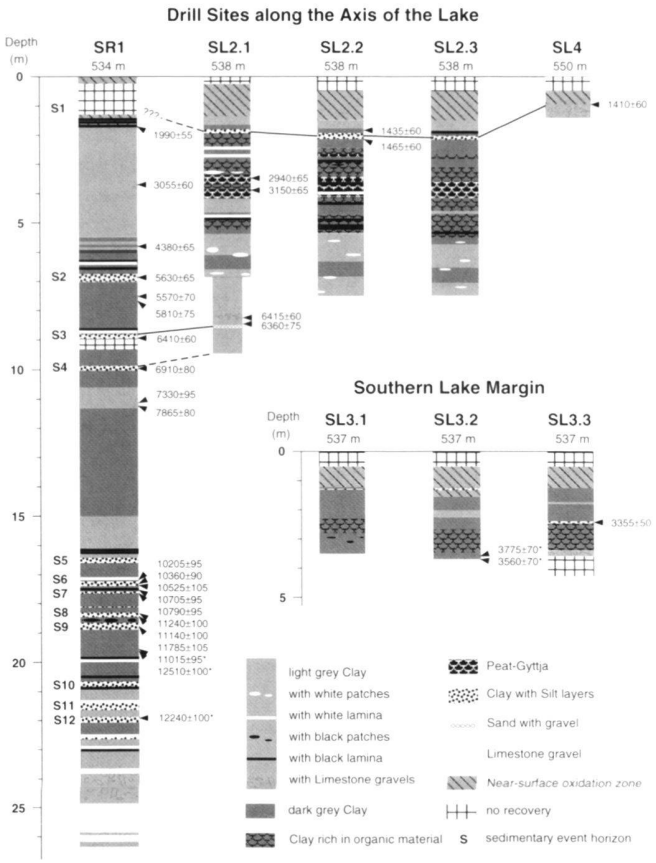

Fig. 9. Lithological borehole logs and radiocarbon ages, Lake Seewen. Asterisks mark critical radiocarbon dates.

al. 1976). The floor of the former lake is at an altitude of 535 m a.s.l. in the western part of the valley. Depth contours for the former lake basin, based on the refraction seismic survey, give a maximum thickness for the sedimentary infill in the range 20 to 24 m in the westernmost part of the lake close to the rock bar (SR1 in Fig. 2). The lake basin is strongly asymmetric, with the greatest depth close to the rock bar of *Welschhans*, decreasing gradually upstream. Together with the boreholes, the refraction seismic depth contours allow an estimate of the volume of the maximum capacity of the lake basin. A top water level for the lake of 550 m a.s.l., which is close to the altitude of the *Welschhans* saddle (551 m), provides an estimate of about $23 \cdot 10^6$ m^3 for the maximum volume of the lake, of which lake deposits occupy about $13 \cdot 10^6$ m^3.

Drilling campaign and lake sediments (Table 1)

With the exception of drill site SL3 (Fig. 2), all boreholes were placed along the centre line of the lake basin. For the older ram drills, no detailed descriptions are available, only a note about the thickness of the lake deposits. In the most recent drilling campaign, started in September 1997, eight boreholes in a further four locations were completed: one commercial ram drill at SR1, one Livingstone drill at SL4, and a pattern of three Livingstone drills at each of the other two locations SL2 and SL3 (Fig. 2). With the exception of boreholes SL2.2 and SL2.3 (at drill site SL2), all drills appear to have reached the base of the lake deposits but could not prove bedrock. Table 1 gives the most important details of the drilling programme.

Summary lithological profiles for the boreholes are given in Fig. 9. The deepest borehole SR1 with a final depth of 26.8 m, passed through more than 3 m of coarse grained debris below a depth of 23.6 m. Drills SL2.1 , SL3.1, SL3.2 and SL4 also reached coarse grained gravel debris. Fragments within the debris are not rounded and consist mainly of limestone. This debris is also locally rich in loam and SR1 even has some thin clay layers (between 26.15–26.35 m). These characteristics are most clearly seen in SR1 and suggest that this debris originated by frost weathering processes and may have been reworked, thus being transported over short distances before being deposited in periglacial conditions. In the boreholes in the shallower part of the lake, this material is more likely to be Holocene talus. As indicated earlier, the Fulnau landslide would not have been able to supply much debris into the lake basin which was well-protected from the landslide by the *Welschhans* rock bar. Therefore, the basal debris deposits which extend for a considerable distance are not considered to contain landslide material.

The lake sedimentary sequences are dominated by grey clay-like deposits with varying amounts of sand, silt and organic material. A summary of particle size analyses is listed in Table 2. A change to a light brown colour (indicating the oxidation zone) is restricted to the topmost 1.5 m of the cores. Occasionally, the whole sequence contains dark and light patches and thin layers. The black and dark grey layers and patches are rich in dispersed organic material or concretionary Fe-Mn. The white laminae and patches consist partly of *Seekreide* (lake chalk). In SL2, between 2 and 5 m depth, there appeared to be gyttja-type sediments rich in plant fibres, leaves and roots. These deposits indicate a low stand of the lake level

Table 2. Summary of particle size analyses for typical lake deposits.

Drill	Depth (m)	Sand (%)	Silt (%)	Clay (%)
SR1	17.31	25	40	35
SR1	18.35	42	29	29
SR1	18.66	52	25	23
SL2.1	1.01	1	49	50
SL2.1	1.50	1	39	60
SL2.1	2.50	10	61	29
SL2.1	3.80	24	48	28
SL2.1	4.99	5	43	52
SL2.1	5.99	2	63	35
SL2.1	7.05	4	62	34
SL2.1	8.00	9	60	31
SL2.1	9.26	3	52	45
SL3.1	1.00	1	51	48
SL3.1	1.66	3	53	44
SL3.1	2.75	6	58	36
SL4	0.85	18	47	35

during the time of deposition. Also, in the lower sections of the SL3 boreholes, high amounts of organic material are present mainly as wood fragments, twigs and roots. SR1 and SL4 are essentially free of concentrations of organic material. Single large angular pebbles embedded in fine-grained clay are frequent in SR1 below 17 m, although they are seen occasionally further up in SR1 and SL2.2 and SL2.3 (in the last two boreholes at a depth of about 7 m). These fragments are interpreted as "dropstones", because they are embedded in a low energy clay matrix (Fig. 10). This can be explained by stones lying on or embedded in ice or within root bales of floating trees, becoming released during decay. Particularly in the younger parts of the cores, root bales have been envisaged as an possible transport medium, because dropstones can frequently be seen together with organic macro remains and enrichments of dispersed organic material in the sediments.

A correlation between the different drill profiles has been attempted on the basis of thin, slighty more silty-sandy layers, which are called "event horizons" numbered between S1 to S12 (Fig. 9). It could well be that these event horizons are related to exceptional floods, storms or a sudden change of the lake level or shaking by earthquakes. Such severe environmental changes could have triggered subaquatic slumping and dewatering, which may explain some of the features seen in these event horizons, e.g. S5. The investigations into the origin of these events are in progress and will be the subject of a future publication.

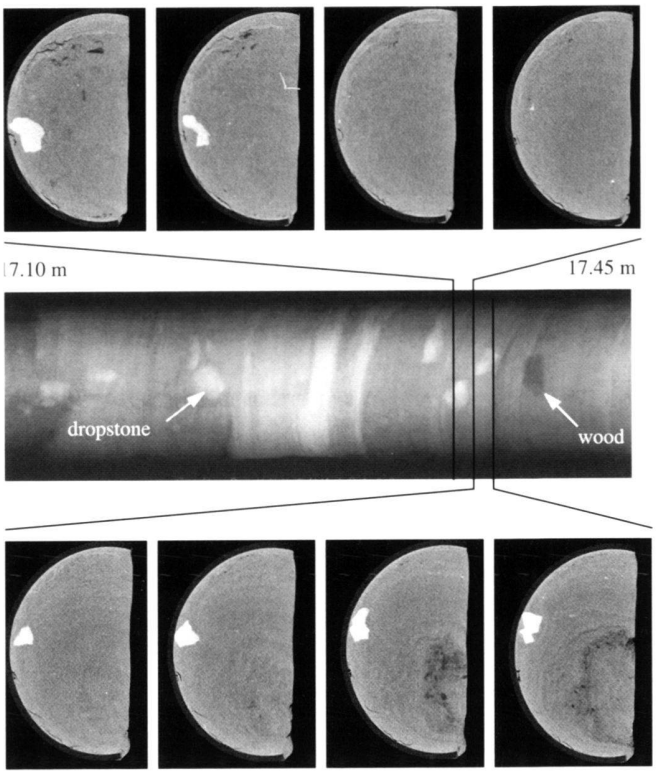

Fig. 10. X-ray image for the SR1 core between 17.10-17.45 m and x-ray tomographic images showing eight cuts through two drop-stones and their embedding relationships seen in half cores. The x-ray parameters for the tomographic images are: 450 kV, 2 mA, slice spacing: 2.5 mm, pixel size: 0.15 mm, grey scaling: dark for low density, bright for high density.

Chronology

Two different methods could be used to provide age constraints: radiocarbon dating and pollen analyses. Together, these two methods supply information about the onset of lake sedimentation and, consequently, for the timing of the Fulnau landslide which dammed the river Seebach, impounding former Lake Seewen. The evolution of the lake and environmental changes from the Late Pleistocene through the Holocene are documented in these chronological records, particularly the onset of sedimentation in different parts of the lake, lake level fluctuations, changing sedimentation rates and vegetation history.

Radiocarbon dating

Altogether 31 samples from the cores of the boreholes SR1, SL2.1, SL2.2, SL3.2 and SL4 were taken and prepared for accelerator mass spectrometry (AMS) radiocarbon dating. Plant

Table 3. Summary of radiocarbon age datings.

Drill Hole	Lab code [UZ-]	Depth (m)	Convent. ^{14}C age (BP)	Dendro-Calibrated dates from Cumulative probability [BC/AD] 1σ-Range	2σ-Range	$\delta^{13}C$ [‰]	Material
SR1	4139	1.70	1990±55	37 BC - 77 AD	126 BC - 143 AD	-25.5	Macroremains
	4161	3.70	3055±60	1376 BC - 1205 BC	1422 BC - 1112 BC	-21.5	Plant fibres
	4138	5.79	4380±65	3126 BC - 2935 BC	3297 BC - 2893 BC	-21.9	Wood
	4160	6.85	5630±65	4533 BC - 4389 BC	4654 BC - 4355 BC	-23.6	Wood
	4137	7.50	5570±70	4473 BC - 4357 BC	4551 BC - 4271 BC	-30.9	Wood
	4176	7.65	5810±75	4759 BC - 4571 BC	4843 BC - 4492 BC	-25.3	Wood
	4254	8.90	6410±60	5408 BC - 5290 BC	5433 BC - 5253 BC	-24.1	Disp. Material
	4136	9.99	6910±80	5841 BC - 5675 BC	5934 BC - 5612 BC	-21.9	Plant fibres
	4163	11.15	7330±95	6259 BC - 6049 BC	6361 BC - 5984 BC	-20.9	Disp. Material
	4164	11.23	7865±80	6911 BC - 6571 BC	6992 BC - 6482 BC	-19.6	Plant fibres
	4141	17.19	10205±95	10161 BC - 9516 BC	10339 BC - 9230 BC	-21.9	Charcoal
	4159	17.31	10360±90	10407 BC -10049 BC	10530 BC - 9755 BC	-24.7	Plant fibres
	4131	17.34	10525±105	10613 BC - 10326 BC	10729 BC - 10151 BC	-21.4	Plant fibres
	4133	17.50	10705±95	10789 BC - 10566 BC	10888 BC - 10449 BC	-19.3	Wood
	4134	17.61	10790±95	10871 BC - 10657 BC	10968 BC - 10547 BC	-22.0	Plant fibres
	4130	18.32	11240±100	11322 BC - 11094 BC	11441 BC - 10990 BC	-19.4	Plant fibres
	4129	18.40	11140±100	11217 BC - 10997 BC	11330 BC - 10894 BC	-21.7	Wood
	4127	18.74	11785±105	11955 BC - 11647 BC	12100 BC - 11518 BC	-31.5	Plant fibres
	4126	19.54	11015±95	11086 BC - 10880 BC	11188 BC - 10781 BC	-18.9	Plant fibres
	4125	19.59	12510±100	12929 BC - 12530 BC	13103 BC - 12373 BC	-26.0	Wood
	4157	21.90	12240±100	12538 BC - 12182 BC	12700 BC - 12038 BC	-20.5	Disp. material
SL2.1	4167	3.46	2940±65	1241 BC - 1036 BC	1354 BC - 945 BC	-26.2	Plant fibres
	4168	3.87	3150±65	1485 BC - 1324 BC	1547 BC - 1232 BC	-24.3	Plant fibres
	4255	8.20	6415±60	5409 BC - 5293 BC	5435 BC - 5257 BC	-21.0	Wood
	4169	8.44	6360±75	5381 BC - 5237 BC	5428 BC - 5104 BC	-20.9	Charcoal
SL2.2	4170	1.84	1435±60	566 AD - 655 AD	474 AD - 720 AD	-24.8	Charcoal
	4171	2.14	1465±60	541 AD - 639 AD	451 AD - 668 AD	-24.6	Wood
SL3.2	4174	3.57	3775±70	2304 BC - 2069 BC	2428 BC - 1983 BC	-25.1	Wood
	4173	3.66	3560±70	1980 BC - 1787 BC	2106 BC - 1707 BC	-23.8	Plant fibres
SL3.3	4256	2.40	3355±50	1686 BC - 1553 BC	1741 BC - 1523 BC	-19.3	Charcoal
SL4	4175	0.90	1410±65	584 AD - 686 AD	504 AD - 766 AD	-25.0	Charcoal

fibres, wood and charcoal particles, as well as macroremains (which cannot be more closely determined than as seeds or bud remains) were picked out by hand. After a standard acid-alkali-acid pretreatment (AAA), the samples were dried and combusted in quartz tubes for further processing. Samples containing dispersed carbon material also required AAA-pretreatment whereby, after each step, material was centrifuged. After pre-treatment, the CO_2 obtained was cracked to graphite. The preparation and pretreatment of the samples for radiocarbon dating was carried out at the ^{14}C-laboratory of the Department of Geography at the University of Zurich. The AMS with the tandem accelerator of the Institute of Particle Physics at the ETH-Hönggerberg was used for dating.

The results of ^{14}C-dating on the organic matter are given in Table 3. The calibrated values were calculated using the program "CalibETH", based on the bidecadal dendro-calibration curve given by Pearson & Stuiver (1993). The oak ring calibration in central Europe goes back as far as 8480 BC (Spurk et al. 1998). Thus, for all the ^{14}C-ages in Table 3 greater or equal to 10429 BP (years before present), calibrations were based on the extended pine tree chronology (back to 11871 BP) (Kromer & Spurk 1998, Spurk et al. 1998) and coral ages (Jöris & Weninger 1998). To avoid the influence of hard water effects on the age determination in this area, where there exists a strong potential for contamination by old carbon from limestones, dating is restricted to terrestrial plant material, e.g. wood and charcoal. Also, for other material there seems to be a direct carbon exchange with the atmosphere as indicated by the $\delta^{13}C$ values (Table 3). As a result, the radiocarbon dates are generally in good agreement with the dates derived from palynostratigraphy, as will be shown later. Therefore, in most cases the age of the material that has been dated seems to be a reliable age for the deposit. However, in the case of wood and charcoal, which can be recycled several times before final sedi-

mentation, a higher age for the embedment layer would result. Wood from an old tree can show age differences of up to several 100 years.

The samples taken for radiocarbon dating were selected to achieve: (a) an even distribution of data points throughout the borehole, (b) dating of event horizons, and (c) stratigraphic correlation among the boreholes. However, in SR1 all the samples which have been taken between 11.23 and 17.19 m could not supply a sufficient amount of organic material and, furthermore, it was not possible to date the base layers of the lake deposits.

In general, the radiocarbon dates show, as one would expect, an increase of age with increasing depth and, where this is not the case, inversion of this trend within the standard deviation. Although there are no indications for contamination or mishandling related to sampling and pretreatment, there are exceptions in SR1 and SL3.2 in the lower sections of the boreholes (Fig. 9). In the key borehole SR1, the problematic ages were resolved by comparison with the palynostratigraphic evidence.The chronology established is then used to estimate sedimentation rates and the onset of sedimentation in the landslide-dammed former Lake Seewen.

Palynostratigraphy

From SR1, altogether 32 samples were taken and chemically treated but only 27 samples could be statistically analysed for their pollen content. The deepest samples between 23.58-26.60 m did not contain pollen that could be assigned to certain species because of corrosion and physical damage. Highest pollen quality was found in the depth interval between 15.90-16.50 m. The pollen data for SL2.1 allow a statistical analysis only for the uppermost five samples down to a depth of 3.5 m, and SL2.2 only for three samples down to a depth of 2 m. In the deeper sections of the three SL2 boreholes, the pollen quality was poor because of corrosion, as is also the case in SL3.1, SL3.2 and SL4.1. Samples showing signs of corrosion have to be handled with care with respect to their statistical relevance, because corrosion may lead to an enrichment of more corrosion resistant pollen grains and, thus, to a biased sample. Therefore, the palynostratigraphical interpretations are restricted to the best record, i.e. SR1, which is the only borehole with a sufficient number of reliable samples and which reached the base of the lake deposits in the deepest part of the lake basin.

Radiocarbon-dated "Standard pollen profiles" for different regions allow the approximate dating of a pollen profile by means of comparison of pollen sequences with those of the standard profile (Burga & Perret 1998). Based on a large number of individual radiocarbon dates, the ages for the pollen zones, which are characterized by a distinct pollen assemblage, are given as conventional, uncalibrated ^{14}C-ages in years BP, starting from 1950 AD.

Fundamentally, the late- and post-glacial vegetation history is similar in most parts of Central Europe and shows a general

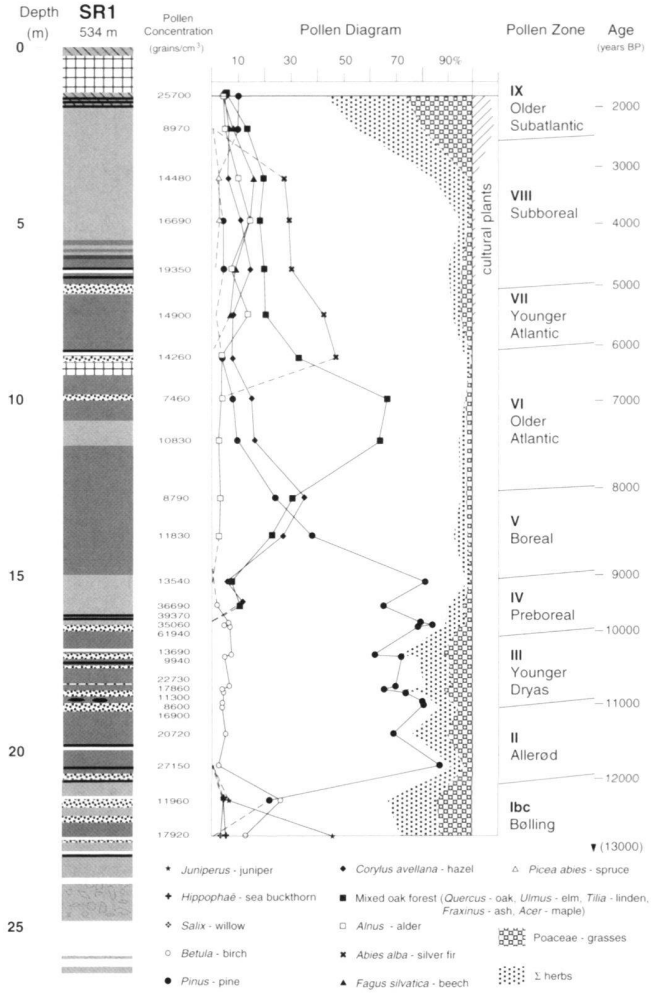

Fig. 11. Palynostratigraphy of the borehole SR1, Lake Seewen.

trend with respect to the chronology of appearance, dominance and retreat or even disappearance of certain species of trees, shrubs or herbs. For the Late Pleistocene and the Early Holocene, dating can reach a remarkable accuracy in the range of 100 to 150 years, if the changes in the vegetation are clearly indicated in the pollen profile. The pollen diagram for SR1 indicates the regional vegetation history of the last c. 13,000 years (Fig. 11): the retreat of birch (*Betula*) and the appearance of pine (*Pinus*) at the beginning of the Allerød, the appearance of mixed oak forest (*Quercus*/oak, *Ulmus*/elm, *Tilia*/linden, *Acer*/maple, *Fraxinus*/ash) and hazel (*Corylus*) at the end of the Preboreal or at the beginning of the Boreal, the hazel maximum and the retreat of pine in the Boreal, the mixed oak forest maximum in the Older Atlantic and the appearance of silver fir (*Abies alba*) at the transition Older/Younger Atlantic. However, independent dating can be achieved only in the older parts of the section based on the

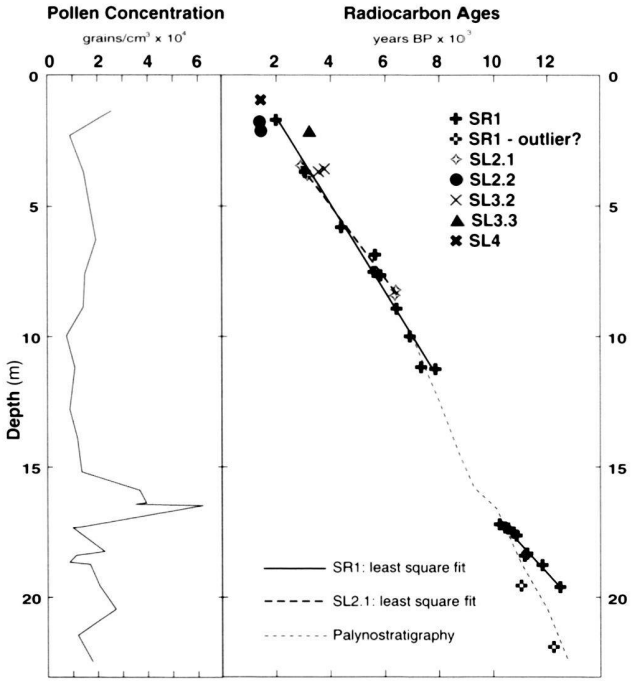

Fig. 12. Relationship of pollen concentration and radiocarbon ages with depth, used to estimate sedimentation rates.

pollen zones alone. The younger section of pollen diagram SR1 (Fig. 11), starting with the Younger Atlantic (from c. 8.5 m upwards), has to be linked directly with the radiocarbon ages from this borehole. The difficulties involved in separating the pollen zones for these younger ages are partly related to an increasing human impact on the vegetation.

The deepest pollen sample with well preserved sporomorphs (at 22.5 m in SR1, Fig. 11) shows a distinct juniper (*Juniperus*) dominance together with high amounts of sea buckthorn (*Hippophaë*) and willow (*Salix*). Together with frequent pollen grains of late-glacial steppe and tundra vegetation, e.g. grass species, *Artemisia*, *Helianthemum*, *Thalictrum* and Chenopodiaceae, this pollen spectrum is typical for the beginning of the Bølling (pollen zone Ibc). Compared with reference profiles from Sewensee, Vosges Mountains, and Nussbaumer Seen, Thurgau (Schloss 1979; Rösch 1983), an age of 12,700 BP can be estimated. Below 22.5 m depth, the pollen conservation is very poor, although some sediments are clays or, at least, rich in clay material. Because the beginning of typical lake sedimentation is about 1.1 m below the deepest pollen sample in SR1, the onset of lake sedimentation cannot be dated exactly. However, based on the assumption that the undatable basal thickness of lake deposits accumulated within a few hundred years, the onset of lake sedimentation can be placed with confidence at the transition Oldest Dryas/Bølling or at the end of the Oldest Dryas around 13,000 to 13,500 BP.

Sedimentation rates

Minimum sedimentation rates, ignoring consolidation of sediments with depth, have been calculated using the radiocarbon and pollen ages. From the Younger Atlantic upwards (from a depth of about 8.5 m in SR1), the sedimentation rates from both methods will be identical, because the pollen ages are directly linked to the radiocarbon ages for SR1. Based on the radiocarbon ages of SR1, the sedimentation rate in the upper 12 m is about 1.6 mm/a. No significant deviation is observed. For SL2.1 only four radiocarbon dates are available, indicating a sedimentation rate of 1.4 mm/a between 6,400 and 2,900 BP, i.e. the late Older Atlantic and the late Subboreal. For the other boreholes, the few data available do not allow an individual sedimentation rate to be calculated. All the relevant information are presented in Fig. 12, including those for boreholes with a limited number of radiocarbon ages. Linear regression curves are based on the data of SR1 and SL2.1. An average minimum sedimentation rate between the early Older Atlantic and the Older Subatlantic of 1.5 mm/a is documented, again without considering consolidation. Because of insufficiant amounts of organic material between 11.23 and 17.19 m, sedimentation rates cannot be calculated from radiocarbon ages. The sedimentation rate of the Late Pleistocene can be based on ten radiocarbon dates. Although there is some scatter in the results, the best fit to eight of the data points supplies a minimum sedimentation rate in the range of about 1 mm/a for the depth interval 17–20 m.

Based on radiocarbon ages alone, it appears that the minimum average sedimentation rate of 1.5 mm/a in the upper Holocene section is about 50% higher than the rate of 1 mm/a in the Pleistocene section. With these sedimentation rates, the deposition of the uppermost 12 m of the profile represents about 8,000 years, and the section between 17–20 m a further 3,000 years, i.e. altogether 15 m of sediment within 11,000 years. If, on the basis of the pollen profile, it is assumed that the lake sedimentation started about 13,500 BP, then the remaining 8.6 m of lake deposits have to be deposited within 2,500 years with an average sedimentation rate of 3.4 mm/a. Independent evidence for varying sedimentation rates is given by the pollen concentration data (Fig. 11 and 12). This is because variations not only depend on the pollen production and the distribution of the contributing vegetation, but are controlled largely by the sedimentation rate such that high sedimentation rates will correlate with low pollen concentrations and vice versus. The pollen concentration between 9.98 and 15.20 m depth show little variation around 10,000 pollen/cm^3. This value is slightly lower than that of the overlying section, perhaps indicating slightly higher sedimentation rates between 10-15 m. The section starting at a depth of 17.31 m down to the limit of pollen sampling at a depth of 22.5 m, shows a larger scatter compared to the section above. This may indicate that Late Pleistocene sedimentation conditions were less stable, with sedimentation rates changing within short time intervals. At least, there are no indications that might point to a possible

higher sedimentation rate and thus significantly lower pollen concentrations. The only exception is the section between 15.9 and 16.5 m where significantly higher pollen concentration values are recorded. However, these higher pollen concentrations point to a short time period of even lower sedimentation rates compared to the average sedimentation rates in the neighbouring core sections. Supposing that the assumptions given for the estimation of the sedimentation rates based on the pollen concentrations are true and that there has been no secondary selective corrosion of pollen grains, then the results indicate that sedimentation rates are unlikely to exceed 3 mm/a.

Taking the pollen record (Fig. 11) as a basis for constraining the minimum average sedimentation rates (Fig. 12), then the sedimentation rate between 10 and 15 m should be about 2.6 mm/a and about 2.1 mm/a in the section below 17 m. However, the value of 2.1 mm/a for the Pleistocene section is more than twice as high as the radiocarbon dating-based sedimentation rate. Here, the palynostratigraphic sedimentation rate for the Pleistocene section is considered to be more likely, because other interpretations do not fit the inferred values for the onset of lake sedimentation.

To conclude, the sedimentation rates of Lake Seewen can be summarized as follows: the minimum average sedimentation rate is about 1.5 mm/a down to a depth of about 10 m, increasing to 2.6 mm/a down to about 15 m and then decreasing to 2.1 mm/a down to the onset of lake sedimentation, only interrupted by a very short-term interval of exceptionally low sedimentation rates between 15.9 and 16.5 m.

Landslides and lake evolution

Former Lake Seewen was impounded by an early failure within the Fulnau area. The geological and hydrological conditions for the creation of the Fulnau landslide have been described above. The events which may have triggered this landslide are not known. The most likely triggering mechanisms are considered to be periods of exceptional precipitation or earthquakes (Adams 1981, Eisbacher & Clague 1984, Keefer 1984, Schuster et al. 1986). Based on the available age constraints, the landslide event occurred in a time of changes in climate and vegetation at the end of the Pleistocene (Bølling), when permafrost melted and the landscape was not completely covered by dense vegetation. Exceptional hydrological conditions must have occurred during this time interval, which could be regarded as factors contributing in the creation of landslides along the northern slope of the *Homberg* mountain and elsewhere in the Jura Mountains, e.g. in the Doubs river valley where cliff collapse impounded *Lac des Brenets* about the same time (Bichet et al. 1999, Schardt 1903). However, the late Pleistocene and early Holocene in Switzerland is believed to be a period of enhanced earthquake activity in the vicinity of the formerly glaciated Alpine area during ice-isostatic rebound and tectonic readjustments.

In general, landslide impoundments do not last for a long time. Schuster et al. (1986) report that 59% of such lakes fail within 1 month, 91% within 1 year, and that the most important mechanism of failure is overtopping and erosion. Because Lake Seewen survived for approximately 13,500 years, exceptional conditions must have been established. These conditions seem to be related to the nature of the landslide dam, the nature of the debris and to the hydrology of the Seebach catchment. The first phase of the Fulnau landslide is believed to have occurred along a steeply incised gorge cut by the river Seebach into the eastern flank of the *Welschhans* anticline. Gorge collapse started when the river Seebach undercut the base of the *Rauracien* limestones and the abutment of the *Homberg* mountain was weakened. Short-distance sliding of large blocks and debris from the near-side cliff was sufficient to close the gorge along its western and central part. At its eastern upstream end, the gorge remained largely intact where it has passed through the stable rock bar at the western end of the lake basin. Blocks and debris reached this eastern end, filling this part of the gorge. However, the present limit of these blocks indicates that not much, if any, debris passed over the rock bar into the lake basin. Landslide dams which are most prone to failure consist mainly of fine grained material (Schuster et al. 1986). Blocky material of the Fulnau type is less likely to be removed during overtopping, although finer material could be removed creating leakage pathways. From these considerations it is believed that the survival of the dam was largely due to the fact that the rock bar was still largely intact and large blocks were involved in the closure of the gorge.

The size of the catchment for Lake Seewen may have contributed to the long-term stability of the impoundment, with an area of only about 18 km^2. Long term precipitation measurements in the surroundings of Seewen give values of about 1200 mm/a. The total water volume supplied by precipitation would be in the range of $21.5 \cdot 10^6$ m^3 in a year. The water volume probably will be reduced by 50% or more due to evaporation, transpiration and infiltration; the last being important because of leakage potential in this karstic area. With this water volume, the lake basin, which originally had a volume of about $23 \cdot 10^6$ m^3 before sediment infill, would need about 2 years to be filled. This amount of water is unlikely to lead to conditions severe enough to damage the rock bar and landslide dam. Only during flood events would there have been potential for erosion. Leakage from the lake basin is realistic, because the gorge infill is blocky and the rock exposures in the lake basin show small karstic features, like the *Hägenloch* ponor. The loss of water in the lake basin was probably higher during the early stages of lake evolution when the floor of the basin was not covered by silty and clayey lake deposits. As shown by Magny (1992), and Magny & Richoz (1998), significant changes in the humidity during the Holocene caused lake level changes in the Jura region. Compared with the present day climate, several periods with low lake level stands indicate "dry" phases with low precipitation. Accordingly, it is considered likely that the lake level remained low for a long time, because of low precipitation, a high potential for leakage through the landslide dam and subsurface flow out of the lake basin.

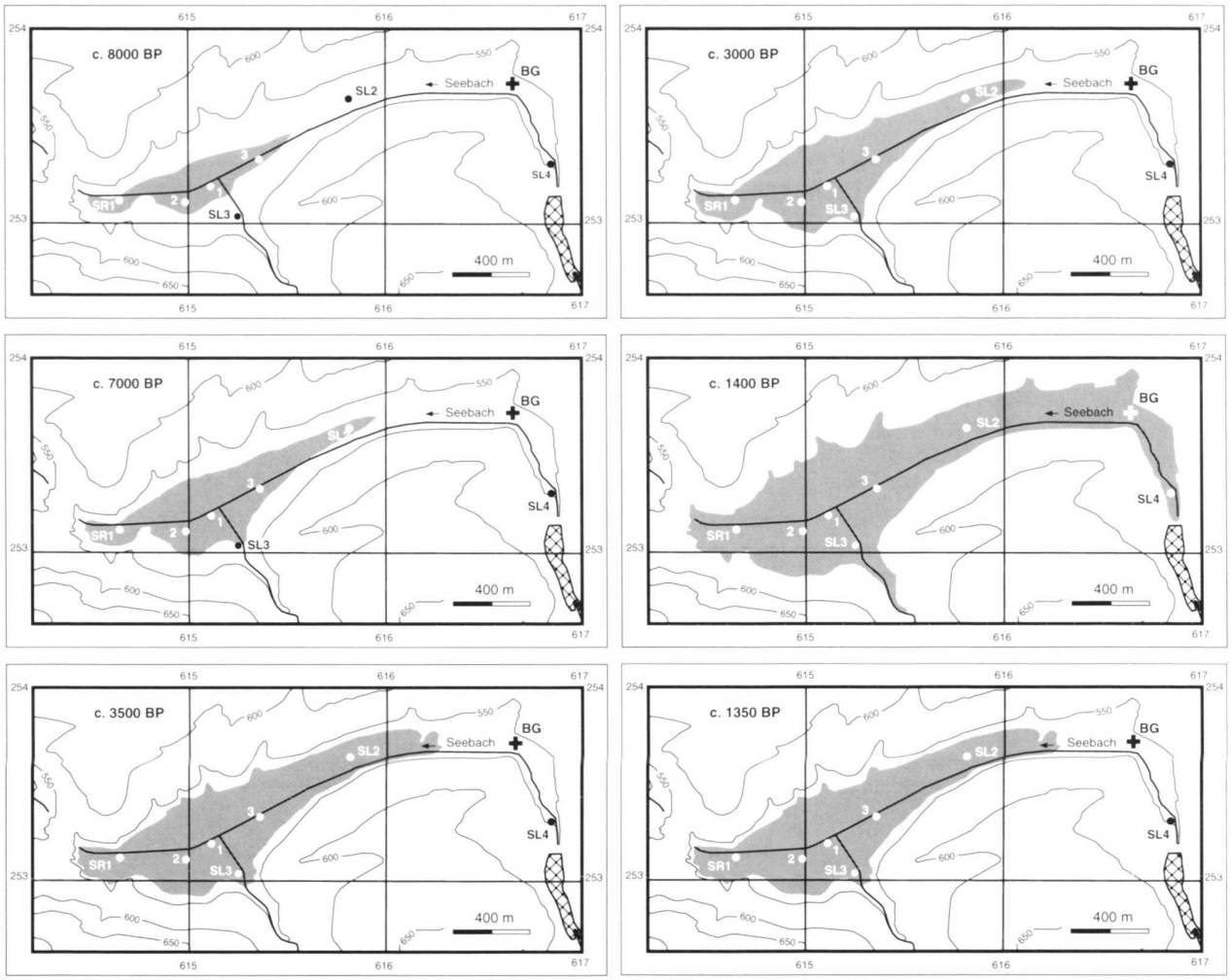

Fig. 13. Lake level fluctuation reconstructions, Lake Seewen. Boreholes are indicated: 1-3, SL2-SL4, SR1. BG: burial ground.

Using the onset of lake sedimentation in the different boreholes and inferred phases of low lake level stands, as indicated by peat-gyttja deposits, it is most likely that during the early stages of the lake evolution (c. 8000 BP) the lake only covered a small area close to the western end of the basin (Fig. 13). Around 7,000 BP, lake sedimentation started at SL2, and around 3,500 BP at SL3. By c. 3,000 BP, there are signs of a lake level fall as indicated by peat-gyttja deposits in SL2 and abundant wood fragments in SL3. This is probably related to a drier period, as discussed above Magny (1992), and Magny & Richoz (1998). The highest lake level stand was reached as late as 1,400 BP (about 600 A.D.), when Lake Seewen extended as far upstream as SL4 near the Baslerweier. The reason of the highest stand is not known for certain. It is possible that the younger small rock fall northwest of the *Welschhans* saddle extended southwards and elevated the maximum lake level slightly. However, the material of this rock fall is susceptible to erosion and, therefore, any elevated lake stand would not last for long. Another possiblility is that human activity may have modified the topography of the *Welschhans* saddle.

After the highest lake level of c. 1400 BP, the lake level fell within a very short time. It is known that Alemannic settlers used the far eastern end of the lake basin as a burial ground (BG in Fig. 13), where graves were dug in lake deposits as deep as 1 m below ground level at that time. The E-W orientation of the graves, the artefacts buried with the corpses and the known onset of Alemannic settlement in northern Switzerland all indicate an age of between mid 7th and earliest 8th century AD, most likely between 650and 680 AD, i.e. only 50 to 100 years after Lake Seewen reached its maximum extension. At this time, the lake level must have been around 540 m a.s.l., probably staying at this level until the final drainage of the lake in the late 16 th century.

The lake history thus appears to be one of continuous transgression, modified by drier or wetter periods, but mostly controlled by the increasing sealing of the lake floor and infill

of the lake basin by mainly clay deposits. These deposits not only reduced the potential for loss into the possibly karstified subsurface but also reduced the volume available for occupation by water. Overtopping of the rock bar and landslide dam seems not to have taken place until the later stages of lake evolution. However, the presence of some cemented debris at the western edge of the *Welschhans* saddle close to the western portal of the *Seeloch* gallery may indicate an escape route (Fig. 5).

The lake basin continues to evolve and further landslides are likely to occur in this area. As can be seen during exceptional flood events, large areas of the valley can be flooded, e.g. most years during late spring and early summer. Also, further cliff collapse west of the Fulnau landslide at the base of the *Riesenberg*, similar to those which happened in the past, could destabilise the remaining limestone slab of the northern slope of the *Riesenberg*. This slab has a free face to the east, i.e. the western edge of the Fulnau landslide and also to the north towards the Mühlebach valley. The crest of the *Homberg-Wisig* anticline is already exposed down to the *Oxford* marls and the western margin of the block is weakened by a fault. This would indicate a high potential for further large-scale landslide events in the Fulnau region.

Acknowledgements

This project was made possible by the support of Prof. Domenico Giardini (ETH, Geophysik) and funding by the ETH and Universität Zürich. We gratefully acknowledge the assistance in the field by Kurt Ruch of the Universität Bern (Geobotanik), Walter Künzle and Urs Gerber (ETH Zürich) for assistance with core logging, also Prof. Hans Laubscher (Universität Basel) for discussing the most recent results of his geological mapping in the region, and Dr. Christoph Wüthrich (Universität Basel) for the particle size analyses. We are also grateful for the support and provision of information by the landowner (Industrielle Werke Basel), especially by Werner Moser, and the cooperation of local farmers. Institut für Geophysik, ETH Zürich, contribution no. 1131.

REFERENCES

ADAMS, J. 1981: Earthquake-dammed lakes in New Zealand. Geology 9, 215–219.

ANNAHEIM, H. & BARSCH, D. 1963: Geographischer Exkursionsführer der Schweiz. Gempenplateau und angrenzende Teilregionen. Geographica Helv. 18, 241–267.

BARSCH, D. 1968: Periglaziale Seen in den Karstwannen des Schweizer Juras. Regio Basiliensis IX/1, 115–134.

BICHET, V., CAMPY, M., BUONCRISTIANI, J.-F., DIGIOVANNI, CH., MEYBECK, M. & RICHARD, H. (1997): Variations in sediment yield from the Upper Doubs River carbonate watershed (Jura, France) since the late-glacial period. Quaternary Res. 51 (3), 267–279.

BITTERLI-BRUNNER, P. & FISCHER, H. 1988: Erläut. geol. Atlas Schweiz 1 : 25000, Blatt 1067 Arlesheim. Landeshydrologie und -geologie, 66 p.

BURGA, C.A. & PERRET, R. 1998: Vegetation und Klima der Schweiz seit dem jüngeren Eiszeitalter. Ott Verlag, Thun, 832 p.

BUXTORF, A. 1901: Geologie der Umgebung von Gelterkinden im Basler Tafeljura. Beitr. geol. Karte Schweiz, NF 11, 106 p.

COROMINAS, J. 1996: The angle of reach as a mobility index for small and large landslides. Can. Geotech. J. 33, 260-271.

EISBACHER, G.H. & CLAGUE, J.J. 1984: Destructive mass movements in high mountains: Hazard and management. Geol. Surv. Can. Paper 84–16, 230 p.

FRENZEL, B., PÉCSI, M. & VELICHKO, A.A. 1992: Atlas of paleoclimates and paleoenvironments of the northern hemisphere – late Pleistocene/Holocene. Hungarian Acad. Sci., Gustav Fischer Velag, Budapest, Stuttgart, 153 p.

HAEBERLI, W., SCHNEIDER, A. & ZOLLER, H. 1976: Der „Seewener See": Refraktionsseismische Untersuchung an einem spätglazialen bis frühholozänen Bergsturz-Stausee im Jura. Regio Basiliensis XVII (2), 133–142.

JÖRIS, O. & WENINGER, B. 1998: Extension of the ^{14}C calibration curve to ca. 40,000 cal BC by synchronizing Greenland $^{18}O/^{16}O$ ice core records and north Atlantic foraminifera profiles: a comparison with U/Th coral data. Radiocarbon 40 (1), 495–504.

KEEFER, D.K. 1984: Landslides caused by earthquakes. Bull. Geol. Soc. Am. 95, 406-421.

KOCH, R., LEHNER, E., WAIBEL, A. & MÜHLBERG, M. 1936: Geologischer Atlas der Schweiz 1 : 25000, Blätter 96 Laufen, 97 Bretzwil, 98 Erschwil, 99 Mümliswil. Geologische Kommission der Schweiz.

KROMER, B. & SPURK, M. 1998: Revision and tentative extension of the tree-ring based ^{14}C calibration, 9200-11,8855 CAL BP. Radiocarbon 40 (3), 1117–1125.

LAUBSCHER, H. 1998: Der Ostrand des Laufenbeckens und der Knoten von Grellingen: Die verwickelte Begegnung von Rheingraben und Jura. Eclogae geol. Helv. 91, 275–291.

MAGNY, M. 1992: Holocene lake-level fluctuations in Jura and the northern subalpine ranges, France: regional pattern an climatic implications. Boreas 21, 319–334.

MAGNY, M. & RICHOZ, I 1998: Holocene lake-level fluctuations in Lake Seedorf, southern Swiss Plateau. Eclogae geol. Helv. 91, 345–357.

PEARSON, G.W. & STUIVER, M. 1993: High-precision bidecadal calibration of the radiocarbon time scale, AD 1950–500BC and 2500–6000 BC. Radiocarbon 35(1), 1–23.

RÖSCH, M. 1983: Geschichte der Nussbaumer Seen (Kanton Thurgau) und ihrer Umgebung seit dem Ausgang der letzten Eiszeit aufgrund quartärbotanischer, stratigraphischer und sedimentologischer Untersuchungen. Mitt. Thurg. Natf. Ges. 45, 3–110.

SCHARDT, H. 1903: Note sur l'origine du lac des Brenets. Bull. Soc. neuchât. Sci. Nat. 32, 312–324.

SCHLOSS, S. 1979: Pollenanalytische und stratigraphische Untersuchungen im Sewensee. Ein Beitrag zur spät- und postglazialenVegetationsgeschichte der Südvogesen. Diss. Bot. 52, Vaduz, 138 p.

SCHUSTER, R.L., ASCE, F. & COSTA, J.E. 1986: A perspective on landslide dams. In: Landslide dams: processes, risk, and mitigation (Ed. by SCHUSTER R.L.). Geotechnical Spec. Publ. 3, 1–20.

SENN, A. 1928: Über die Huppererde von Lausen und das geologische Alter der Zeininger Bruchzone. Eclogae geol. Helv. 21, 163–180.

SPURK, M., FRIEDRICH, M., HOFMANN, J., REMMELE, S., FRENZEL, B., LEUSCHNER, H.H. & KROMER, B. 1998: Revisions and extension of the Hohenheim oak and pine chronologies: new evidence about the timing of the Younger Dryas/Preboreal transition. Radiocarbon 40 (3), 1107–1116.

Manuscript received September 16, 1999
Revision accepted June 29, 2000